

## MalariaCount: An image analysis-based program for the accurate determination of parasitemia

Selena W.S. Sio<sup>a</sup>, Weiling Sun<sup>a</sup>, Saravana Kumar<sup>b</sup>, Wong Zeng Bin<sup>b</sup>, Soon Shan Tan<sup>a</sup>,  
Sim Heng Ong<sup>b</sup>, Haruhisa Kikuchi<sup>c</sup>, Yoshiteru Oshima<sup>c</sup>, Kevin S.W. Tan<sup>a,d,\*</sup>

<sup>a</sup> Laboratory of Molecular and Cellular Parasitology, Department of Microbiology, Yong Loo Lin School of Medicine, National University of Singapore, Singapore

<sup>b</sup> Vision and Image Processing Laboratory, Department of Electrical and Computer Engineering, Faculty of Engineering,  
National University of Singapore, Singapore

<sup>c</sup> Graduate School of Pharmaceutical Sciences, Tohoku University, Sendai 980-8578, Japan

<sup>d</sup> National Malaria Reference Centre, National University of Singapore, Singapore

Received 4 April 2006; received in revised form 29 May 2006; accepted 31 May 2006

Available online 11 July 2006

### Abstract

Malaria is a serious global health problem and rapid, precise determination of parasitemia is necessary for malaria research and in clinical settings. Manual counting by light microscopy is the most widely used technique for parasitemia determination but it is a time-consuming and laborious process. The aim of our study was to develop an automated image analysis-based system for the rapid and accurate determination of parasitemia. We have developed, for the first time, a software, MalariaCount, that automatically generates parasitemias from images of Giemsa-stained blood smears. The potential application and robustness of MalariaCount was tested in normal and drug-treated in vitro cultures of *Plasmodium falciparum*. The results showed a tight correlation between MalariaCount and manual count parasitemia values. These findings suggest that MalariaCount can potentially be used as a tool to provide rapid and accurate determination of parasitemia in research laboratories where frequent, large-scale, efficient determination of parasitemia is required.

© 2006 Elsevier B.V. All rights reserved.

**Keywords:** *Plasmodium*; Malaria; Parasitemia; Imaging; Tool; Program

### 1. Introduction

Malaria, caused by protozoan parasites of the genus *Plasmodium*, is the most serious and widespread parasitic disease of humans. It affects at least 200 to 300 million people every year and causes an estimated 3 million deaths per annum (Shiff, 2002; Phillips, 2001). Of the four species known to infect humans, *Plasmodium falciparum* is the most virulent and contributes to the majority of deaths associated with the disease (Hisaeda et al., 2005).

Many current research efforts have been focused on new approaches to control the spread of malaria (Contreras et al.,

2004). Our understanding of *P. falciparum* biology was accelerated when continuous in vitro culture of the parasite was established (Trager and Jensen, 1976). In in vitro drug susceptibility and antibody-mediated invasion inhibition assays, parasitemia values can respectively indicate if the parasite growth is disrupted or merozoite invasion of the RBC is prevented. Approaches to determining susceptibility of *P. falciparum* to an anti-malarial compound include manual microscopic enumeration of Giemsa-stained thick and thin blood films, flow cytometry, quantitation of incorporated tritium-labeled hypoxanthine, or ELISA-based detection of certain malaria-specific molecules (Noedl et al., 2003). Among these, light microscopy is the most widely used technique for parasitemia determination (Hanscheid, 1999). However, microscopy is a time-consuming process and relies on the expertise of the technician (Payne, 1998).

A standardized automated image analysis software would circumvent these limitations associated with manual parasitemia

\* Corresponding author. Laboratory of Molecular and Cellular Parasitology, Department of Microbiology, Yong Loo Lin School of Medicine, National University of Singapore, 5 Science Drive 2, Singapore 117597, Singapore. Tel.: +65 6516 6780; fax: +65 6776 6872.

E-mail address: [mictank@nus.edu.sg](mailto:mictank@nus.edu.sg) (K.S.W. Tan).

determination. Such approaches have been adopted successfully for blood cell morphology identification (Tatsumi and Pierre, 2002), but have not been extensively developed for malaria-infected RBC. To date, there have been no reports on the application of image analysis software for the determination of human malaria parasitemia from blood films.

In the current study, we have developed image-analysis based software that has the capacity to automatically generate parasitemia values from in vitro cultures of *P. falciparum*. Such a system would be an invaluable contribution to studies that are heavily dependent on parasitemia determination.

## 2. Materials and methods

### 2.1. Parasite culture, drug assay and Giemsa staining

*P. falciparum* strain 3D7 (Walliker et al., 1987) was cultured in vitro using the method of Trager and Jensen (1976) following modifications described previously (Smith et al., 2000). Briefly, cultures were grown at 5% hematocrit in 25 ml tissue culture flasks in complete medium that consisted of RPMI 1640 supplemented with 4.2% v/v 5% NaHCO<sub>3</sub> and 0.5% w/v albumax (Gibco-BRL). Cultures were gassed with 3% O<sub>2</sub>, 5% CO<sub>2</sub> and 92 % N<sub>2</sub>, and incubated at 37 °C. In the drug assays, the cultures were treated with 17 µM and 35 µM of chloroquine diphosphate (Sigma-Aldrich) and 0.7 nM and 3.5 nM of febrifugine (extracted and purified from dried roots of *Dichroa febrifuga* at the Graduate School of Pharmaceutical Sciences, Tohoku University, Japan, as previously described by Takaya et al., 1999). Thin blood films from cultures were made and stained with Giemsa (Merck, Germany). Briefly, working solutions of Giemsa were made by adding 100 µl stock solution to each milliliter of distilled water. Dried thin blood films were fixed with methanol for 30 s, poured off and stained with Giemsa for 20 min. The stain was rinsed off with tap water for 10 s. Upon drying, slides were used immediately or mounted (DePex, Hopkin and Williams, England) and stored for future use.

### 2.2. Image acquisition

Stained thin blood films were viewed under an oil-immersion objective (100×) using an image analysis setup which consisted of a light microscope (Olympus BX60) coupled to a 3-CCD color video camera (JVC, Japan) which was in turn connected to a personal computer. Digital images were randomly captured with the aid of a software (Synoptics Acquis 2.59) and stored. Captured images were used as raw data for the development of MalariaCount (below) and for subsequent drug assays.

### 2.3. Image analysis

MalariaCount, an image analysis software, using MATLAB (Version 6.5.1, MathWorks, USA), was designed at the Vision and Image Processing Laboratory, National University of

Singapore, to differentiate infected from uninfected RBC, and to generate parasitemia values. Its algorithm can be divided into the following four sequential stages: (1) edge detection, (2) edge linking, (3) clump splitting, and (4) parasite detection.

#### 2.3.1. Edge detection

The images are first subjected to a preprocessing step which involves the enhancement of the image contrast via adaptive histogram equalization (Karel, 1994). We then identified the boundary edges of RBCs with the aid of the following edge correlation coefficient:

$$E_i = \frac{\langle b_i - \bar{b}_i + c\gamma, g \rangle}{\|b_i - \bar{b}_i + c\gamma\| \|g\|} \quad (1)$$

where  $i$  denotes the image pixels,  $g$  is the edge detector,  $\bar{b}_i$  is the average luminance of the  $n \times n$  local neighbourhood vector  $b_i$  (in column-wise format) centered at  $i$ ,  $\gamma$  is a regularization parameter estimated using the measure of median absolute deviation (MAD) (Donoho and Johnstone, 1995) and  $c$  is a scaling constant empirically chosen to be 3 which is similar to the value used in the references (Olivo-Marin, 2002; Murtagh and Starck, 2000).

A pixel belongs to the boundary edge of the RBCs if its corresponding  $|E_i|$  (ranges from 0 to 1) exceeds the empirically determined threshold of 0.2. The correlation coefficient in (1) is robust under contrast and luminance variations in the images.

#### 2.3.2. Edge linking

The resultant edge contours need to be linked together at their terminal points to form closed boundaries around the RBCs. The terminal points are identified using 20 different  $3 \times 3$  masks shown in Fig. 1. Image pixels whose local neighborhoods match any one of these masks are identified as terminal points. Neighboring boundary edge contours are linked together if their terminal points are in close proximity and the curvature at the linkage is similar to those of RBCs.

#### 2.3.3. Clump splitting

The clumping together of RBCs adversely affects the accuracy of the parasitemia. Therefore, a clump splitting method (Kumar et al., 2005) is implemented in order to split clumps of two or more RBCs into constituent cells of interest. First, the deepest boundary pixels, i.e., the concavity pixels in a clump, are detected using a fast and accurate scheme. Next, concavity-based rules are applied to generate the candidate split lines that join pairs of concavity pixels. A figure of merit is then used to determine the best split line from the set of candidate lines. This process is repeated on the split clumps until no further split lines can be found. Experimental results, as shown in Fig. 2, indicates that the method is robust and accurate.

#### 2.3.4. Parasite detection

The parasites (Fig. 3A–4) are characterized by regions within the RBCs (excluding the RBC boundaries) corresponding to

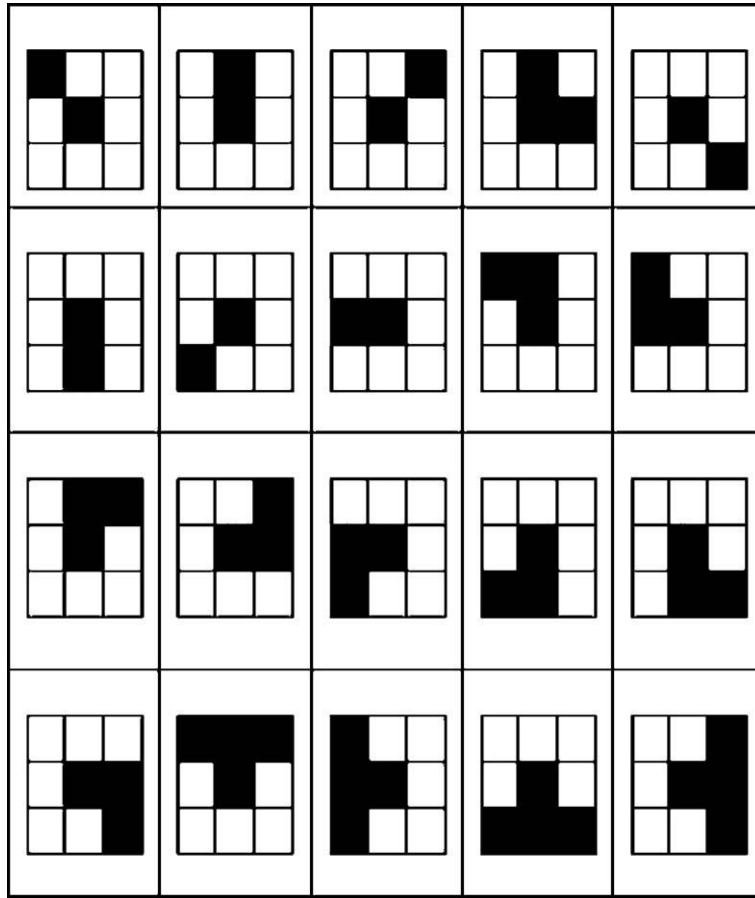


Fig. 1. Masks used in the identification of end points.

large edge response magnitude  $|E_i|$  (Fig. 3A-2). We identify the regions within RBCs via the use of a binary mask as follows. First, a binary filling operation is performed on the closed boundary contour of the RBCs to yield results as shown in Fig. 3A-3. Next, the filled regions are eroded by applying a disk-shaped structural element of radius two, in order to obtain the inner regions of the RBCs where the parasites are located.

#### 2.4. Experimental details

Altogether, we analyzed 76 thin blood smears of varying parasitemias and these smears were studied in two parts. The first part involved analyzing 20 thin blood smears, randomly chosen from a collection of smears made during routine maintenance of malaria in vitro cultures. From these 20 smears,

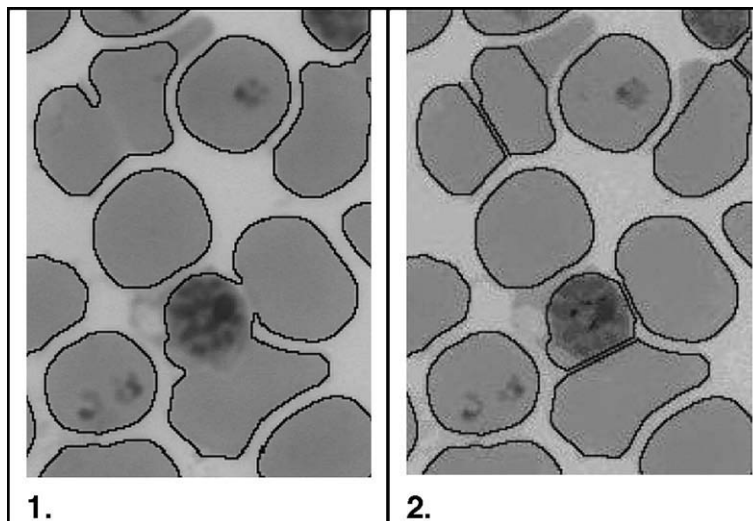


Fig. 2. RBC boundary outlines. (1) Before clumping splitting. (2) After clump splitting.

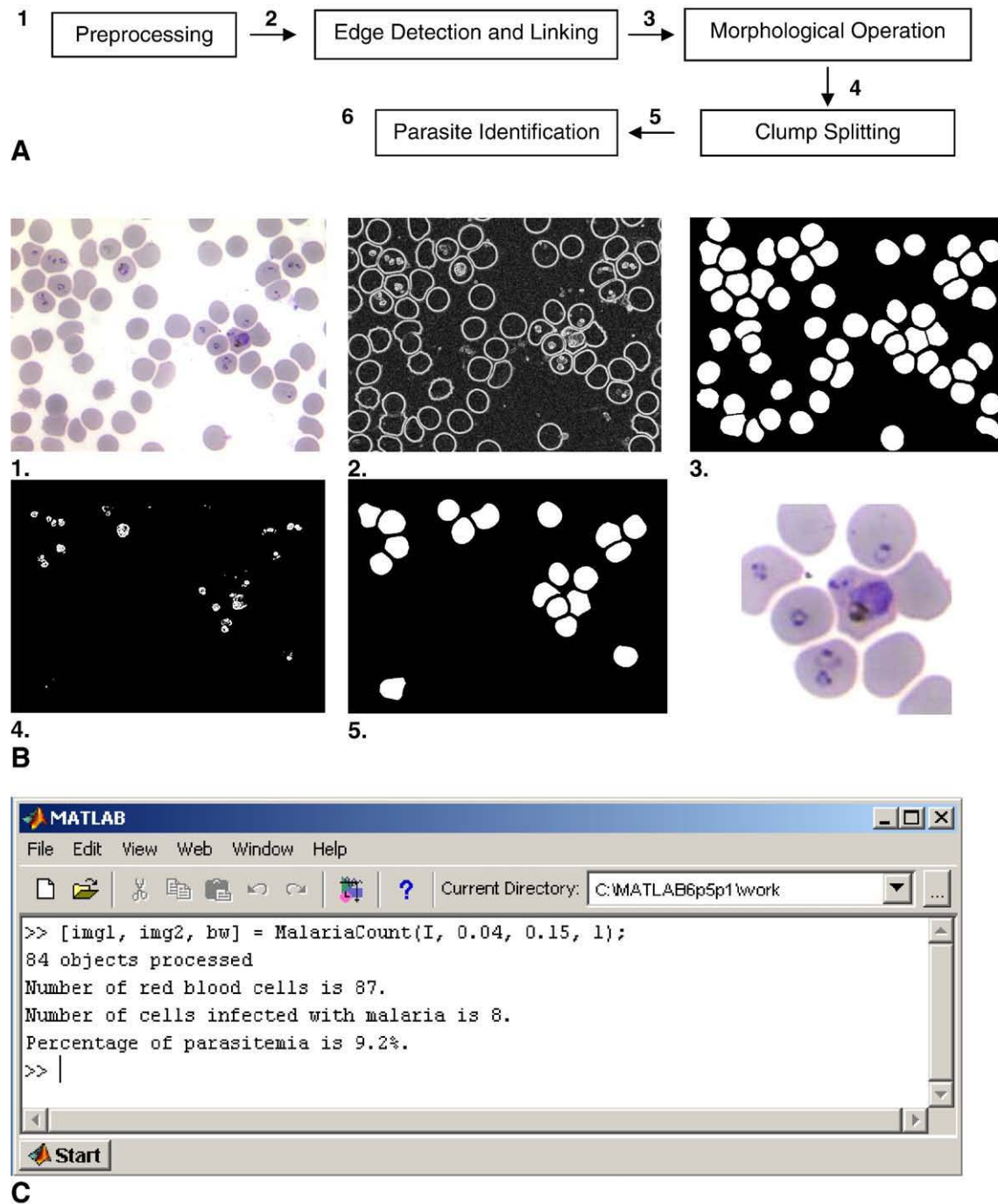


Fig. 3. Image processing steps and output of Giemsa-stained thin blood films. (A) Flowchart of the preprocessing steps. The various stages of processing are graphically illustrated in (B) in the following sequence: (1) Original image, (2) edge response map, (3) binary mask of RBCs after edge detection, linking and clump splitting *E*, (4) parasitic regions detected, (5) binary mask of infected RBCs. Note that cells touching the edge of the image are automatically discounted from the software. Bottom-right panel shows enlarged view of representative infected cells used in this study. The command line execution of the MalariaCount software and the textual output are shown in (C). The software requires the pre-processed image and some segmentation parameters as inputs. It then generates the textual results together with a set of images during the various stages of processing. The program code can be found in the Supplementary Material Section of the manuscript's online version.

which contained infected blood of varying parasitemia, 200 images were captured, comprising approximately 15,000 RBCs. These images were processed through MalariaCount and parasitemias generated were recorded. Parasitemia from each captured image were also manually analyzed by trained

personnel and used as a reference to which MalariaCount parasitemia were compared. To standardize our manual counts, cells touching the periphery of each captured image were not counted, as the software was programmed to exclude them. For controls, images from a smear of uninfected RBC were also

captured. A major problem in both laboratory and field studies is the high person-to-person differences when counting blood smears. Hence, we next investigated person-to-person variability in parasitemia determination by manual counting in comparison to MalariaCount reproducibility. Five representative images each from three smears of varying parasitemia were examined by two trained personnel and % parasitemias were noted (manual count 1, manual count 2). These same images were processed through MalariaCount twice for reproducibility (MalariaCount 1, MalariaCount 2). Results were tabulated as manual count 1 vs manual count 2 and MalariaCount 1 vs MalariaCount 2. Approximately 500 RBCs were counted for each of the 3 smears used.

The second part investigated 56 thin blood smears obtained from chloroquine and febrifugine sensitivity assays (28 smears for each assay). A total of 196 images comprising approximately 16,000 RBCs were processed through the software for each drug assay. Parasitemia from each smear was subsequently manually obtained by trained personnel, with no prior knowledge of the software-generated parasitemia values of each smear. These assays were essentially carried out in a single blind fashion to ensure objectivity. At least 2000 erythrocytes were counted for each smear. Manual counts obtained in the single blind test were

used as a reference to which MalariaCount parasitemia were compared. Untreated infected RBCs were used as controls.

### 2.5. Statistical analysis

Correlation between manual counts- and MalariaCount-generated parasitemia was determined by linear regression analysis. Scatter plots of parasitemia values obtained by both methods was analyzed using the statistical functions in SigmaPlot (Ver 8.0, SPSS Inc.) and JMP (Ver 6.0, SAS Inc.).

## 3. Results

### 3.1. Software processing

The image processing software, MalariaCount, was designed using the MATLAB platform with the main steps outlined in Fig. 3A. Briefly, this involved the detection of the RBC using edge detection, binary morphology and clump splitting routines. Subsequently, parasite infection within each RBC is identified based on the characteristic edge properties of the parasite. The graphical and textual results of MalariaCount are shown in Fig. 3B and C, respectively.

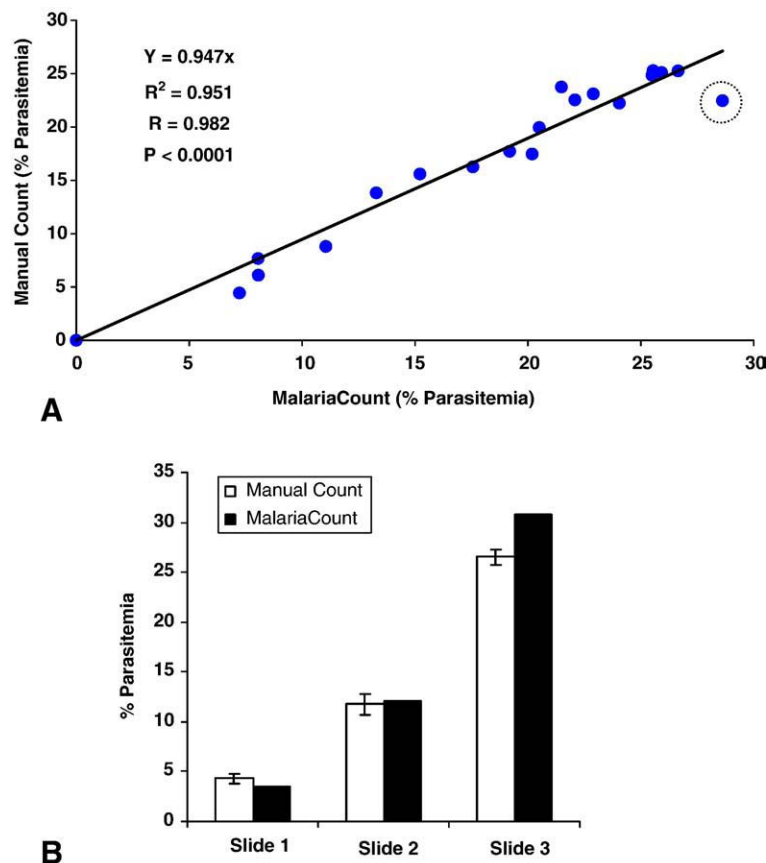


Fig. 4. Establishment of MalariaCount using normal in vitro malaria cultures. (A) Scatter plots for the association of parasitemia determined by manual counts and the software MalariaCount. 20 thin blood smears, 200 images and 15,000 RBCs were investigated. (B) Histogram of % parasitemia values obtained by manual counting and MalariaCount for investigating variability in parasitemia determination. Approximately 500 RBCs were examined in each smear and parasitemia was determined. Results from manual counting for all 3 smears showed variability whereas results from MalariaCount consistently showed no variability. Error bars=standard deviation.



### 3.2. Manual counts vs MalariaCount

Scatter plot analysis of % parasitemia revealed good correlation between manual count and MalariaCount (Fig. 4A). However, there was significant variation between manual counts and MalariaCount parasitemia in one slide (circled outlier, Fig. 4A). When analyzed further, it was observed that this blood smear contained predominantly poorly stained, overlapping and lysed blood cells, which contributed to inaccuracies of the system. In general, inaccuracies arose mainly due to fields that contained overlapping or lysed cells, which resulted in MalariaCount's overestimation of parasitemia. To test this, 10 fields each of well and poorly separated cells from various slides were subjected to MalariaCount. The results revealed that instances of inaccurate parasitemia (average difference in parasitemia  $2.04 \pm 2.86\%$ ) were a result of poor cell separation, while fields containing well separated cells had small deviations from manual counts (average difference in

parasitemia  $0.25 \pm 0.18\%$ ) (results not shown). Investigations into person-to-person variability in parasitemia determination by manual counting in comparison to MalariaCount reproducibility revealed that there was marked person-to-person variation. In contrast, MalariaCount gave consistently identical results for all images processed (Fig. 4B).

Figs. 4A and 5A and B depict the correlation between manual counts and MalariaCount by scatter plot analysis of blood smears obtained from routine malaria in vitro cultures, and chloroquine and febrifugine-treated cultures, respectively. There was good correlation between manual and MalariaCount for cultures without drug treatment ( $n=20$ ;  $R=0.982$ ,  $P<0.0001$ ) (Fig. 4A). MalariaCount for drug assays with chloroquine ( $n=28$ ;  $R=0.958$ ;  $P<0.0001$ ) and febrifugine ( $n=28$ ;  $R=0.928$ ;  $P<0.05$ ) also showed tight correlations and significant  $p$ -values when compared with manual counts obtained from the single blind tests (Fig. 5A and B, respectively). In the case of chloroquine, there was a dose- and time-dependent decline in parasitemia as

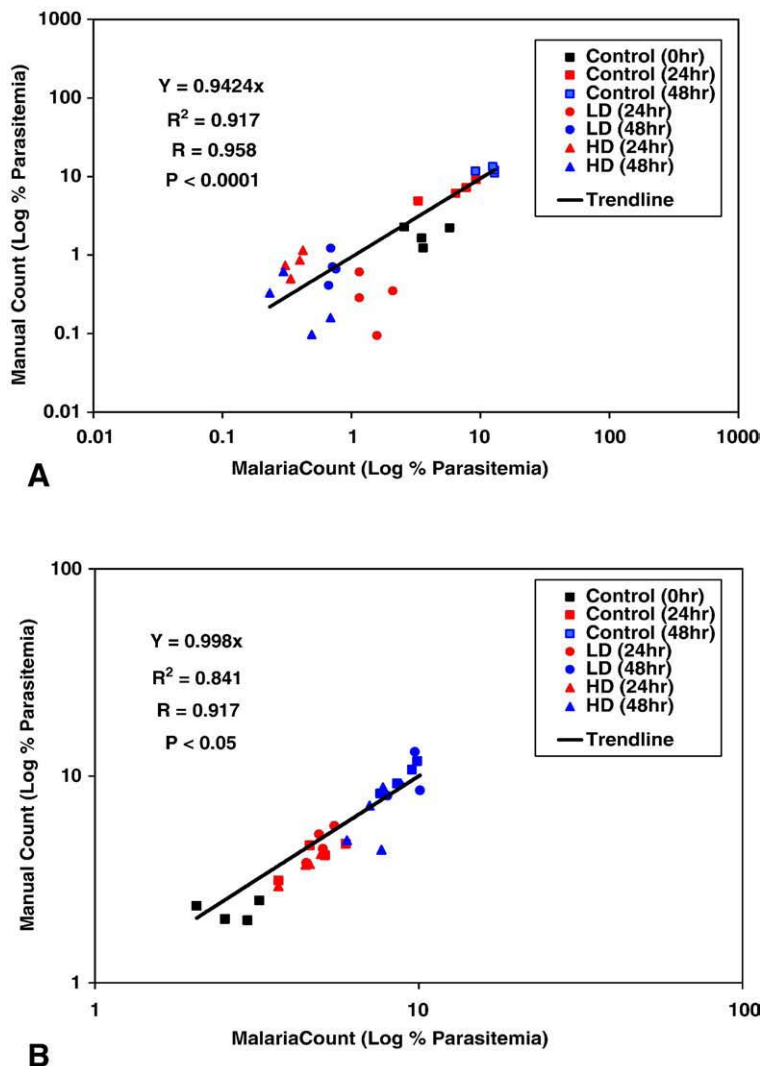


Fig. 5. Validation of MalariaCount with drug-treated in vitro cultures. Scatter plots for the association of parasitemia determined by manual counts and the software MalariaCount with chloroquine (A) and with febrifugine treatment (B). 28 thin blood smears, 196 images, and 16,000 RBCs were investigated for each conditions (LD, low dose; HD, high dose).

chloroquine is known to inhibit in vitro growth of chloroquine sensitive 3D7 strain of *P. falciparum* (Pradines et al., 2002).

#### 4. Discussion

In the current study, we have developed an image analysis software, MalariaCount, which could potentially be employed for the routine determination of parasitemia from thin blood smears of in vitro cultures. The application of MalariaCount was validated using in vitro drug-treated cultures of *P. falciparum*.

The design of the image analysis software for enumeration of malaria-infected RBC is based on several steps. The preprocessing step involves the enhancement of the image contrast via adaptive histogram equalization (Karel, 1994). The next process, edge detection, serves to obtain the boundaries (or contours) of all RBC objects in each image (field). The resultant contours may be broken, and therefore, an edge-linking process is applied in order to form a set of closed cell contours. Subsequently, binary morphological techniques are used to ensure that enclosed regions with distinctly different sizes and shapes from those of RBC are removed. Irregularities due to image artifacts along the contours of RBC regions are also smoothed. The regions enclosed by these contours may comprise clumps of overlapping RBC. Hence, MalariaCount has a clump splitting routine that separates these regions into their constituent objects. Finally, the edge correlation coefficient and binary morphology serve to differentiate infected from uninfected RBCs.

In certain situations, we noticed that small specks within RBCs, such as those caused by particulate matter from the stain or from fragments of released hemazoin, would lead to false interpretation of an infected RBC. To obviate this problem, a thresholding feature was incorporated to discount particulate artifacts that are smaller than the nuclei of early ring forms. The segmentation step was able to distinguish RBCs that were slightly overlapping. However, this did not work for cells that displayed greater overlaps in situations where multiple cells were touching or if the blood cells had lysed. Other inaccuracies may be attributed to the fact that MalariaCount ignores particles or clumps that are connected to the borders of the scanned images. The final step of the software involves the identification of the parasite regions based on their edge attributes. Overall, the software worked very well for well-stained and well-separated cells and is able to accurately process cells exhibiting partial overlaps.

The software could be run from the command window of MATLAB. With the current setup, and depending on the complexity of the image, it takes approximately 30 s to process a single image (results not shown). The software could also be instructed to process images in batches of several hundred to automatically generate parasitemia values without the need for supervision. This also eliminates factors such as user fatigue and lack of standardization that are often associated with manual enumeration. We are in the process of encoding the algorithm in a low-level computer language such as C or C++ that would allow processing speeds to increase by about a hundredfold.

The average difference between automated and manual counts for well-segmented cells was approximately 0.2% parasitemia. This is generally acceptable for studies involving drug assays and antibody-mediated inhibition of invasion, which generally seek to assay for larger variations in parasitemia. In addition, the reproducibility of results in single blind tests and variability experiments demonstrates consistency in MalariaCount and show that it is robust. Furthermore, MalariaCount is capable of identifying parasites despite morphological alterations of *P. falciparum* by chloroquine (Jacobs et al., 1988; Oliaro et al., 1989) and febrifugine treatment (current study). The results also show that MalariaCount can be effectively applied to a wide range of % parasitemias as evidenced by chloroquine- and febrifugine-treated cultures. MalariaCount, however, will unlikely work for field studies involving patient samples or for drug/vaccine studies in animal models due to the additional presence of nucleated cells and other factors (e.g., platelets) that will influence the software's reliability.

When mounted on a motorized stage, the algorithm could be modified to automatically screen for and capture well-separated cells to increase the accuracy and efficiency of the system. The thresholding feature ensured that small particulate matter did not give rise to false positives, which improved the specificity of the software. This was evidenced by the output of 0% parasitemia when 10 fields of uninfected RBCs were processed (Fig. 4A).

While this paper was being reviewed, a report describing an automated image processing method for the speciation of malaria on thin smears was published (Ross et al., 2006). This study employed the use of neural networks to differentiate between the four species of human malaria, although the positive predictive values were in the range of 28–81%, depending on the malaria species examined. However, unlike our present study, Ross et al. (2006) did not incorporate a clump-splitting routine into the software, which precluded the generation of % parasitemia values.

We have developed an image-based software, MalariaCount, that characterizes malaria-infected RBC via edge-based parameters. This software can readily be applied to many assays that are heavily dependent of parasitemia determination, and where large variations in values are expected. Further functional enhancements to the software should include identification of different malaria species and parasitic stages.

#### Acknowledgements

This work was supported by the Microbiology Vaccine Initiative Grant (R-182-002-067-731) generously provided by the National University of Singapore. The authors thank Associate Professor Peter Preiser, School of Biological Sciences, Nanyang Technological University, for helpful discussions and Dr. Mark Taylor, National University of Singapore, for critical reading of the manuscript. The authors are grateful to Ms Ng Geok Choo and Mr Ramachandran for help with malaria cultures.

## Appendix A. Supplementary material

Supplementary data associated with this article can be found, in the online version, at [doi:10.1016/j.mimet.2006.05.017](https://doi.org/10.1016/j.mimet.2006.05.017).

## References

- Contreras, C.E., Rivas, M.A., Domainguez, J., Charris, J., Palacios, M., Bianco, N.E., Blanca, I., 2004. Stage specific activity of potential antimalarial compounds measured in vitro by flow cytometry in comparison to optical microscopy and hypoxanthine uptake. *Mem. Inst. Oswaldo Cruz, Rio de Janeiro* 99, 179–184.
- Donoho, D.L., Johnstone, I.M., 1995. Adapting to unknown smoothness via wavelet shrinkage. *J. Am. Stat. Assoc.* 90 (432), 1200–1224.
- Hanscheid, T., 1999. Diagnosis of malaria: a review of alternatives to conventional microscopy. *Clin. Lab. Haematol.* 21, 235–245.
- Hisaeda, H., Yasutomo, K., Himeno, K., 2005. Malaria: immune evasion by parasites. *Int. J. Biochem. Cell Biol.* 37, 700–706.
- Jacobs, G.H., Oduola, A.M., Kyle, D.E., Milhous, W.K., Martin, S.K., Aikawa, M., 1988. Ultrastructural study of the effects of chloroquine and verapamil on *Plasmodium falciparum*. *Am. J. Trop. Med. Hyg.* 39, 15–20.
- Karel, Z., 1994. Contrast limited adaptive histogram equalization. *Graphics Gems IV*, 474–485 (code: 479–484).
- Kumar, S., Ong, S.H., Ranganath, S., Ong, T.C., Chew, F.T., 2005. A rule-based approach for robust clump splitting. *Pattern Recogn.* 39, 1088–1098.
- Murtagh, F., Starck, J.L., 2000. Image processing through multiscale analysis and measurement noise modeling. *Stat. Comput.* 10, 95–103.
- Noedl, H., Wongsrichanalai, C., Wernsdorfer, W.H., 2003. Malaria drug-sensitivity testing: new assays, new perspectives. *Trends Parasitol.* 19, 175–181.
- Olivo-Marin, J.C., 2002. Extraction of spots in biological images using multiscale products. *Pattern Recogn.* 35, 1989–1996.
- Olliaro, P., Castelli, F., Caligaris, S., Druilhe, P., Carosi, G., 1989. Ultrastructure of *Plasmodium falciparum* “in vitro”. II. Morphological patterns of different quinolines effects. *Microbiologica* 12, 15–28.
- Payne, D., 1998. Use and limitations of light microscopy for diagnosing malaria at the primary health level. *Bull. W.H.O.* 66, 621–626.
- Phillips, R.S., 2001. Current status of malaria and potential for control. *Clin. Microbiol. Rev.* 14, 208–226.
- Pradines, B., Alibert, S., Houdoin, C., Santelli-Rouvier, C., Mosnier, J., Fusai, T., Rogier, C., Barbe, J., Parzy, D., 2002. In vitro increase in chloroquine accumulation induced by dihydroethano- and ethenoanthracene derivatives in *Plasmodium falciparum* parasitized erythrocytes. *Antimicrob. Agents Chemother.* 46, 2061–2068.
- Ross, N.E., Pritchard, C.J., Rubin, D.M., Dusé, A.G., 2006. Automated image processing method for the diagnosis and classification of malaria in thin blood smears. *Med. Biol. Eng. Comput.* 44, 427–436.
- Shiff, C., 2002. Integrated approach for malaria control. *Clin. Microbiol. Rev.* 15, 278–293.
- Smith, T.G., Lourenco, P., Carter, R., Walliker, D., Ranford-Cartwright, L.C., 2000. Commitment to sexual differentiation in the human malaria parasite, *Plasmodium falciparum*. *Parasitology* 121, 127–133.
- Takaya, Y., Tasaka, H., Chiba, T., Uwai, K., Tanitsu, M., Kim, H.S., Wataya, Y., Miura, M., Takeshita, M., Oshima, Y., 1999. New type of febrifugine analogues, bearing a quinolizidine moiety, show potent antimalarial activity against *Plasmodium* malaria parasite. *J. Med. Chem.* 42, 3163–3166.
- Tatsumi, N., Pierre, R.V., 2002. Automated image processing. Past, present, and future of blood cell morphology identification. *Clin. Lab. Med.* 22, 299–315.
- Trager, W., Jensen, J.B., 1976. Human malaria parasites in continuous culture. *Science* 193, 673–675.
- Walliker, D., Quakyi, I.A., Wellems, T.E., McCutchan, T.F., Szarfman, A., London, W.T., Corcoran, L.M., Burkot, T.R., Carter, R., 1987. Genetic analysis of the human malaria parasite *Plasmodium falciparum*. *Science* 236, 1661–1666.